© 2015. Published by The Company of Biologists Ltd | Development (2015) 142, 3210-3221 doi:10.1242/dev.124289

RESEARCH ARTICLE

Hsa-miR-30d, secreted by the human endometrium, is taken up by the pre-implantation embryo and might modify its transcriptome

Felipe Vilella[1,*,‡], Juan M. Moreno-Moya[1,*], Nuria Balaguer[1,*], Alessia Grasso[1], Maria Herrero[1], Sebastian Martínez[1], Antonio Marcilla[2] and Carlos Simón[1,3]

ABSTRACT

During embryo implantation, the blastocyst interacts with and regulates the endometrium, and endometrial fluid secreted by the endometrial epithelium nurtures the embryo. Here, we propose that maternal microRNAs (miRNAs) might act as transcriptomic modifier of the pre-implantation embryo. Microarray profiling revealed that six of 27 specific, maternal miRNAs were differentially expressed in the human endometrial epithelium during the window of implantation – a brief phase of endometrial receptivity to the blastocyst – and were released into the endometrial fluid. Further investigation revealed that hsa-miR-30d, the expression levels of which were most significantly upregulated, was secreted as an exosome-associated molecule. Exosome-associated and free hsa-miR-30d was internalized by mouse embryos via the trophectoderm, resulting in an indirect overexpression of genes encoding for certain molecules involved in the murine embryonic adhesion phenomenon – *Itgb3*, *Itga7* and *Cdh5*. Indeed, this finding was supported by evidence *in vitro*: treating murine embryos with miR-30d resulted in a notable increase in embryo adhesion. Our results suggest a model in which maternal endometrial miRNAs act as transcriptomic modifiers of the pre-implantation embryo.

KEY WORDS: Has-miR-30d, Pre-implantation embryo, Endometrial fluid, Embryo adhesion

INTRODUCTION

In 2010, 45 million couples were affected by infertility (Mascarenhas et al., 2012), and this number is expected to rise as child-bearing is increasingly postponed. More than 5 million children have been born through assisted reproduction (Mansour et al., 2014), and research in this area is moving toward the improvement of success rates, and improvement of success rates through a better understanding of embryo and uterine physiology.

The human embryo undergoes complex developmental modifications throughout the pre-implantation period (Niakan et al., 2012), during which it enters the uterine cavity at the blastocyst stage and embeds in the endometrial fluid (EF) (Cross et al., 1994). During the implantation process, the blastocyst regulates the expression and secretion of integrins β3, α4 and α1 (Simón et al., 1997), the interleukin-1 (IL-1) system (De los Santos et al., 1996), chemokines IL-8, MCP-1 and RANTES (Caballero-Campo et al., 2002), leptin (Cervero et al., 2004; González et al., 2000) and hCG (Licht et al., 2001; Paiva et al., 2011) by the endometrial epithelium during the window of implantation (WOI), the period when the endometrium is receptive to a blastocyst. The EF, a viscous fluid secreted by the endometrial glands into the uterine cavity, nurtures the embryo and constitutes the microenvironment in which the first bidirectional dialogue between the maternal endometrium and the embryo occurs during the WOI (Cha et al., 2012, 2013; Thouas et al., 2014; Tranguch et al., 2005).

The developmental origins of adult disease are now recognized to reflect intrauterine conditions during embryonic and fetal life (Turchinovich et al., 2011). Accumulated evidence suggests that the EF serves as the 'uterine milk' (Burton et al., 2007; Khalil et al., 2009) that nurtures the embryo not only during implantation but beyond (Godfrey and Barker, 2001; Kennedy et al., 2007). The EF contains a variety of molecules, including glycodelin (van der Gaast et al., 2009), cytokines (Boomsma et al., 2009; Simón et al., 1996), lipids (Vilella et al., 2013) and proteins (Domínguez et al., 2009; Hannan et al., 2010), but their impacts on embryo physiology and the putative developmental origins of adult diseases are unknown (Barker, 1990).

Of increasing importance to all aspects of human physiology, including development, are microRNAs (miRNAs), the small, 19-22 nucleotide sequences of non-coding RNA that function as regulators of endogenous gene expression (Ambros and Chen, 2007; Bartel, 2004). miRNAs are secreted by cells and incorporated into microvesicles or associated with proteins that protect them from RNase degradation, endowing them with a long half-life (Turchinovich et al., 2011; Yoshizawa and Wong, 2013). These molecules have been implicated in the regulation of the WOI (Altmäe et al., 2010; Kuokkanen et al., 2010; Ng et al., 2013; Sha et al., 2011), decidualization (Estella et al., 2012a,b) and embryo development in humans (Mincheva-Nilsson and Baranov, 2010), and, more recently, embryo implantation in mice (Chen et al., 2015; Kang et al., 2015; Liu et al., 2013; Revel et al., 2011). In the present study, we aimed to elucidate the role of and mechanisms by which maternal miRNAs secreted into the EF act as transcriptomic regulators of the reprogramming of pre-implantation embryos by the maternal intrauterine environment.

RESULTS

Human EF miRNA profile

First, a microarray analysis of RNA transcripts present in EF was conducted to determine the global expression profile; this revealed a large proportion of miRNAs (supplementary material Fig. S1A), as well as a differential expression pattern among the different phases of the menstrual cycle. Thus, to establish a specific analysis, EF samples were classified into the following groups based on the

[1]Fundación Instituto Valenciano de Infertilidad (FIVI), Department of Obstetrics and Gynecology, Universitat de València, Instituto Universitario IVI/INCLIVA, 46980 Valencia, Spain. [2]Departamento de Biología Celular y Parasitología, Facultad de Farmacia, Universitat de València, 46100 Burjassot (Valencia), Spain. [3]Department of Obstetrics and Gynecology, School of Medicine, Stanford University, Palo Alto, CA 94304, USA.
*These authors contributed equally to this work

‡Author for correspondence (felipe.vilella@ivi.es)

Received 12 March 2015; Accepted 30 July 2015

Development (2015) 142, 3210-3221 doi:10.1242/dev.124289

timing of sample collection: early proliferative (EP; days 6-8; *n*=4), late proliferative (LP; days 9-14; *n*=4), early secretory (ES; days 15-18; *n*=4), WOI (days 19-23; *n*=4) or late secretory (LS; days 24-28; *n*=4).

Microarray technology was used to compare the expression of miRNAs in EF during other phases of the menstrual cycle with that exhibited during the WOI. Significance analysis of microarrays (SAM) with a false discovery rate (FDR) correction <5% allowed us to identify differential miRNA expression across the menstrual cycle. Compared with the WOI, nine differentially expressed miRNAs were identified in the EP phase, eight in the LP phase, six in the ES phase and four in the LS phase (Fig. 1A). Bioinformatics analysis to predict the function(s) of these differentially expressed miRNAs primarily targeted cell cycle and endocrine processes (supplementary material Fig. S1B). As shown on the heat map in Fig. 1A, miRNAs tended to be downregulated in the proliferative phase and upregulated in the secretory phase compared with the WOI. Supervised principal components analysis (PCA) revealed that the EF obtained from the WOI was different from EF secreted at different points of the cycle based on miRNA composition (Fig. 1B). Interestingly, hsa-miR-30d was the most differentially secreted maternal miRNA in the EF during the WOI compared with the rest of the menstrual cycle (Fig. 1C). The hsa-miR-30d concentration in the EF during the WOI, corresponding to the time when an embryo would be present in a conception cycle, was 194.68±29.90 nM (Fig. 1D).

Hsa-miR-30d is secreted by the endometrial glands and transported as an exosome-associated molecule

Next, the cellular origin and mechanism of secretion of endometrial miRNAs into the EF were investigated. As miRNAs are usually secreted in exosomes and carried by Argonaut proteins (Valadi

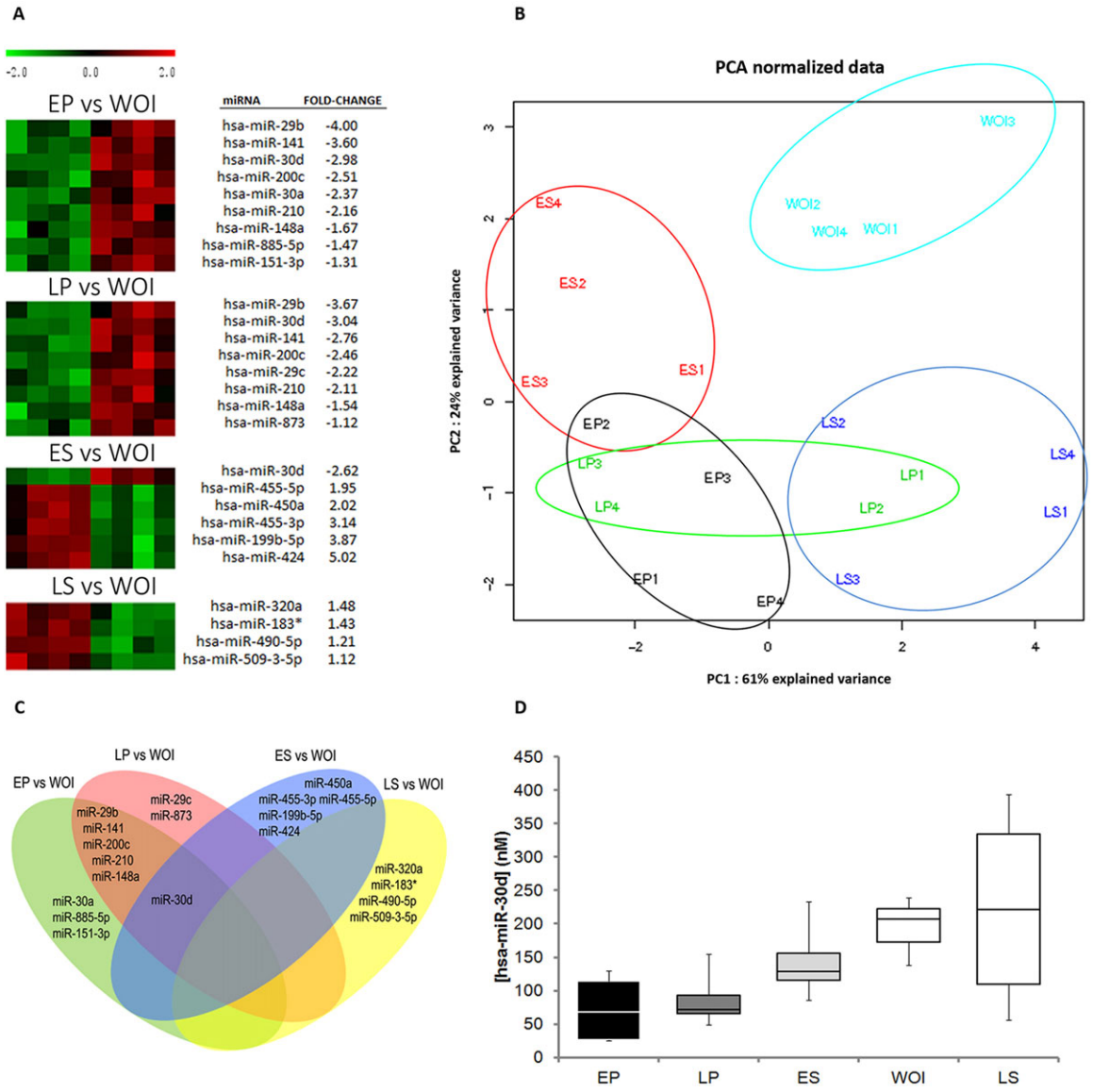

Fig. 1. Study of the specific miRNA profile during the window of implantation (WOI). (A) Heat map of the differential expression of secreted maternal miRNAs during the WOI relative to other phases of the menstrual cycle. (B) Supervised principal components analysis (PCA) to distinguish differentially expressed miRNAs in endometrial fluid (EF) obtained throughout the menstrual cycle relative to the WOI. (C) Venn diagram demonstrating the overlap in expression of miRNAs at different phases of the menstrual cycle, with special attention on hsa-miR-30d in the WOI. (D) Hsa-miR-30d concentration in the EF throughout the menstrual cycle. Boxes represent the first quartile, median and third quartile, and error bars represent maximum and minimum values.

Development (2015) 142, 3210-3221 doi:10.1242/dev.124289

et al., 2007), an initial search for these extracellular vesicles in the human endometrium was performed. To identify exosomes, CD63, a well-known exosome marker (Colombo et al., 2014), was detected by immunochemistry. CD63 staining was observed to be localized in apical and glycocalyx regions of the glandular epithelium during the WOI. By contrast, relatively less intense staining was observed in the ES endometrium, corresponding to the pre-receptive phase (Fig. 2A). Using transmission electron microscopy (TEM),

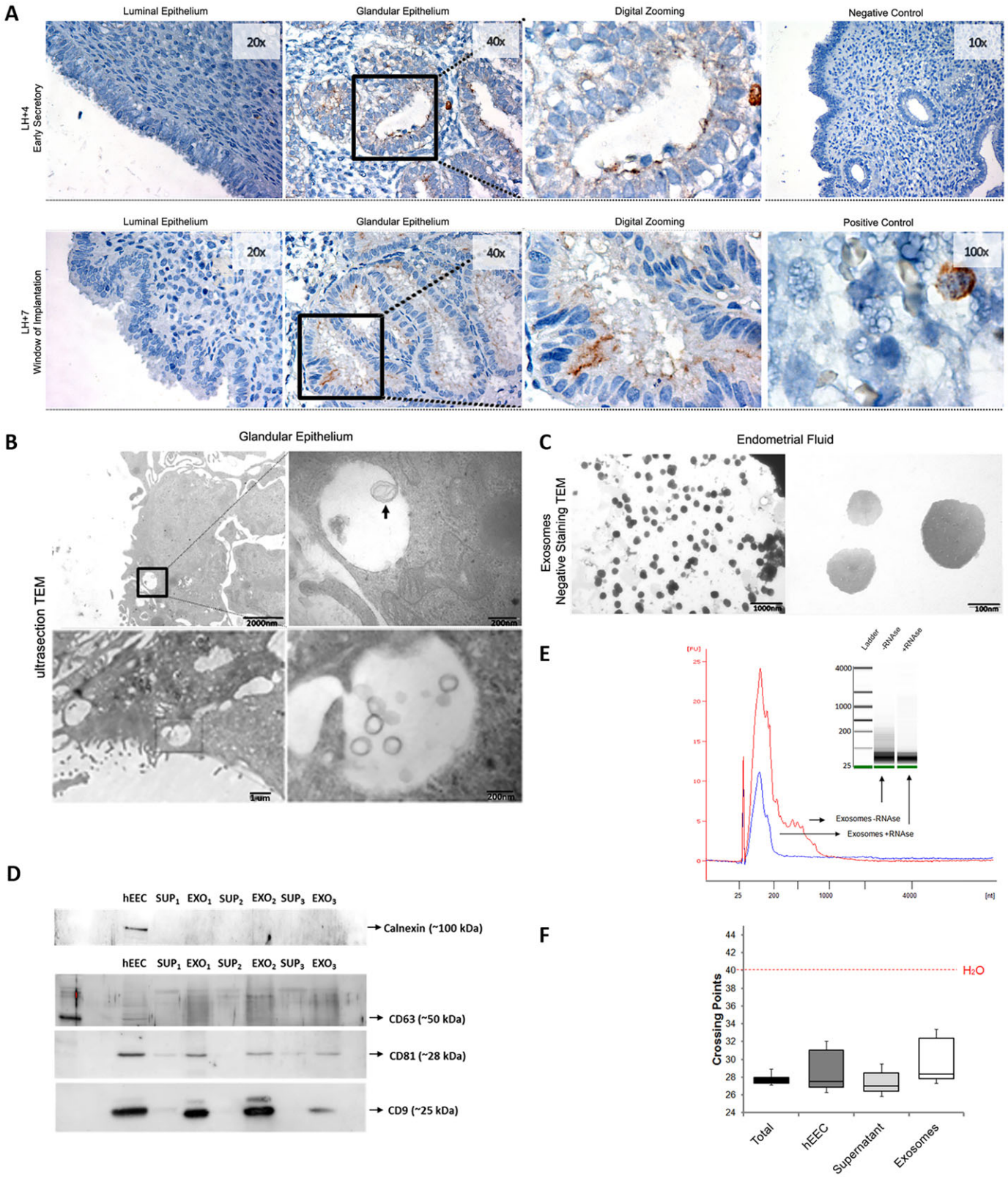

Fig. 2. See next page for legend.

Development (2015) 142, 3210-3221 doi:10.1242/dev.124289

Fig. 2. Identification of the secretion of exosomes loaded with RNA from hEECs into the EF. (A) Immunohistochemical staining of CD63 in the human glandular and luminal epithelium during the early secretory phase (4 days after luteinizing hormone peak; LH+4), the WOI (LH+7) and in the negative (no primary antibody) and positive (immune cell) controls. (B) Transmission electron microscopy (TEM) images of glandular hEECs showing an endosome proximal to the plasma membrane with a small exosome (arrow). Another glandular hEEC shows the same type of endosome compartment in which it is possible to distinguish several exosomes. (C) Electron micrographs of negative staining with uranyl acetate for exosomes purified from EF. (D) Western blot identifying calnexin (negative control) and possible exosome markers CD63, CD9 and CD81 in protein extracts from hEECs, three fractions of exosomes derived from three different human biopsies, and their respective supernatants obtained after ultracentrifugation. (E) Results from a small RNA lab chip assay showing the RNA content of primary hEEC-derived exosomes with or without treatment with RNase A. (F) Crossing points (*y*-axis) for hsa-miR-30d in cells, supernatant, exosomes purified from primary hEEC cultures and total supernatant without depletion of exosomes. The box represents the first quartile, median and third quartile, and the error bars represent maximum and minimum values.

glandular epithelial cells in the secretory phase were verified to have high endosome content, with sizes ranging from 50 to 250 nm (Fig. 2B). These endosomes contained vesicles the size of which was consistent with the exosomes that appear to be secreted into the endometrial cavity. Negative-staining electron microscopy, after ultracentrifugation of human EF, corroborated the presence of these exosomes (Fig. 2C). Western blot analysis showed that the exosome fraction from primary human endometrial epithelial cell (hEEC) culture was positive for the three exosomal tetraspanins CD63, CD81 and CD9 (Colombo et al., 2014; Mathivanan et al., 2011; Ng et al., 2013) and negative for calnexin (Tian et al., 2013) (Fig. 2D).

After verifying that human endometrial epithelium produces and secretes exosomes, in support of Ng et al. (2013), an *in vitro* model of primary hEECs was used to obtain large quantities of exosomes (3.5±1.26 µg of total protein from hEEC-conditioned media). A small RNA LabChip was used to detect the presence of miRNAs within vesicles. RNase treatment did not result in an absence of miRNAs, demonstrating that exosomes protected miRNAs from degradation (Fig. 2E). Among potential miRNAs, hsa-miR-30d was identified in exosomes obtained from hEEC-conditioned media, primary hEECs and exosome-depleted conditioned media (Fig. 2F).

Next, the endogenous production of miR-30d by hEECs and its secretion in exosomes were identified by using a specific custom probe (SmartFlare, Millipore). Each probe consists of a gold nanoparticle conjugated to many copies of the same double-stranded oligonucleotide encoding the target sequence (in this case, hsa-miR-30d). One strand of the oligonucleotide bears a fluorophore (Cy3) that is quenched by its proximity to the gold core. When the nanoparticle contacts its target, the target RNA displaces the fluorophore. The reporter strand, now unquenched, fluoresces and can be detected using any fluorescence detection platform, like a confocal microscope (Fig. 3A; supplementary material Movie 1). A scrambled sequence that does not recognize any target in cells was used as a background control. To delimit the main location of the gold nanoparticles, and, consequently, the one for the hsa-miR-30d, a TEM assay was performed. As the micrographs show, most of these nanoparticles were included inside vesicles (Fig. 3B).

This finding demonstrates that maternal endometrial miRNAs are transported inside exosomes. Taken together, these observations suggest that maternal miRNAs, specifically hsa-miR-30d, are actively produced and secreted from the glandular epithelium into the lumen of the endometrial cavity.

Embryos take up free and/or exosome-associated hsa-miR-30d from the EF

To investigate the hypothesis that the embryo is able to take up free and/or exosome-associated miRNAs from the EF, uptake of free hsa-miR-30d was tested in an *in vitro* mouse model. Day-1.5 embryos (n=30) were cultured for 72 h with 400 nM Alexa 488-labeled scramble miRNA. Uptake by trophectoderm cells was confirmed by immunofluorescence in either the hatched area or the trophectoderm after zona pellucida removal without affecting embryo quality (Fig. 4A; supplementary material Movie 2). The embryos (n=60) were incubated with 50 nM, 100 nM or 400 nM free synthetic miR-30d (to mimic) using scramble miRNA as a negative control, and miR-30d uptake was validated by real-time quantitative PCR (Fig. 4C).

To test the embryo acquisition of exosome-secreted miRNAs, the vesicles isolated from primary hEECs were stained with the exosome membrane marker Vybrant DiO and added to the culture media containing day-4.5 mouse blastocysts (n=15) for 24 h. As seen for free miR-30d, the trophectoderm in the hatched area or after zona pellucida removal exhibited the ability to take up exosomes (Fig. 4B; supplementary material Movie 3). This finding was validated using scanning electron microscopy (SEM) to visualize the trophectoderm surface of exosome-co-cultured embryos (Fig. 4D). Small, rounded vesicles surrounded by microvilli were attached to the apical trophectoderm membrane, close to pores or cell membrane invaginations in treated embryos.

In addition, an *in vitro* assay was performed in which miR-30d-labeled hEECs were co-cultured with unstained mouse embryos. The miR-30d signal was observed to transfer from the hEECs to the trophectoderm of embryos when they were attached to the hEEC monolayer. However, when the attachment was not present, no fluorescence was observed in the embryo. The red signal of miR-30d was evident in embryo cells in the rolling stage, an event confirmed in the adhesion and invasion phases (Fig. 5; supplementary material Fig. S2). These results demonstrate that secreted maternal miRNAs, specifically miR-30d, either free or in exosome-associated form, can be incorporated into the embryo via the trophectoderm.

Hsa-miR-30d secreted by hEECs induces transcriptional and functional embryo modifications

Finally, to demonstrate the functional relevance of this novel maternal tissue-embryo communication mechanism, we investigated the effects of endometrial miRNA uptake on the embryonic transcriptome and phenotype. A gene expression microarray of day-1.5 mouse embryos (n=360, performing triplicates), cultured in the presence of either 400 nM hsa-miR-30d or scramble miRNA for 72 h, revealed an overexpression of ten genes in embryos cultured with miR-30d mimic (Fig. 6A; supplementary material Fig. S3 and Tables S2-7 include all comparisons between the different groups, i.e. non-treated, scramble, mimic miR-30d and inhibitor of miR-30d). These genes were investigated using the web-based tool DAVID (http://david.abcc.ncifcrf.gov/home.jsp) to identify the most likely affected biological processes. The regulated genes were related to cell adhesion, integrin-mediated signaling pathways and developmental maturation (Fig. 6B). The phenotypic effect of this transcriptomic regulation was demonstrated using an *in vitro* model of embryo adhesion (Garrido-Gómez et al., 2012; Martín et al., 2000). Four conditions were compared in six different experiments (15 embryos per condition, n=6): control without miRNA, scramble miRNA, mimic miR-30d and miR-30d inhibitor. After 32 h of co-culture, the presence of mimic miR-30d resulted in an increased rate of embryonic adhesion to the

Development (2015) 142, 3210-3221 doi:10.1242/dev.124289

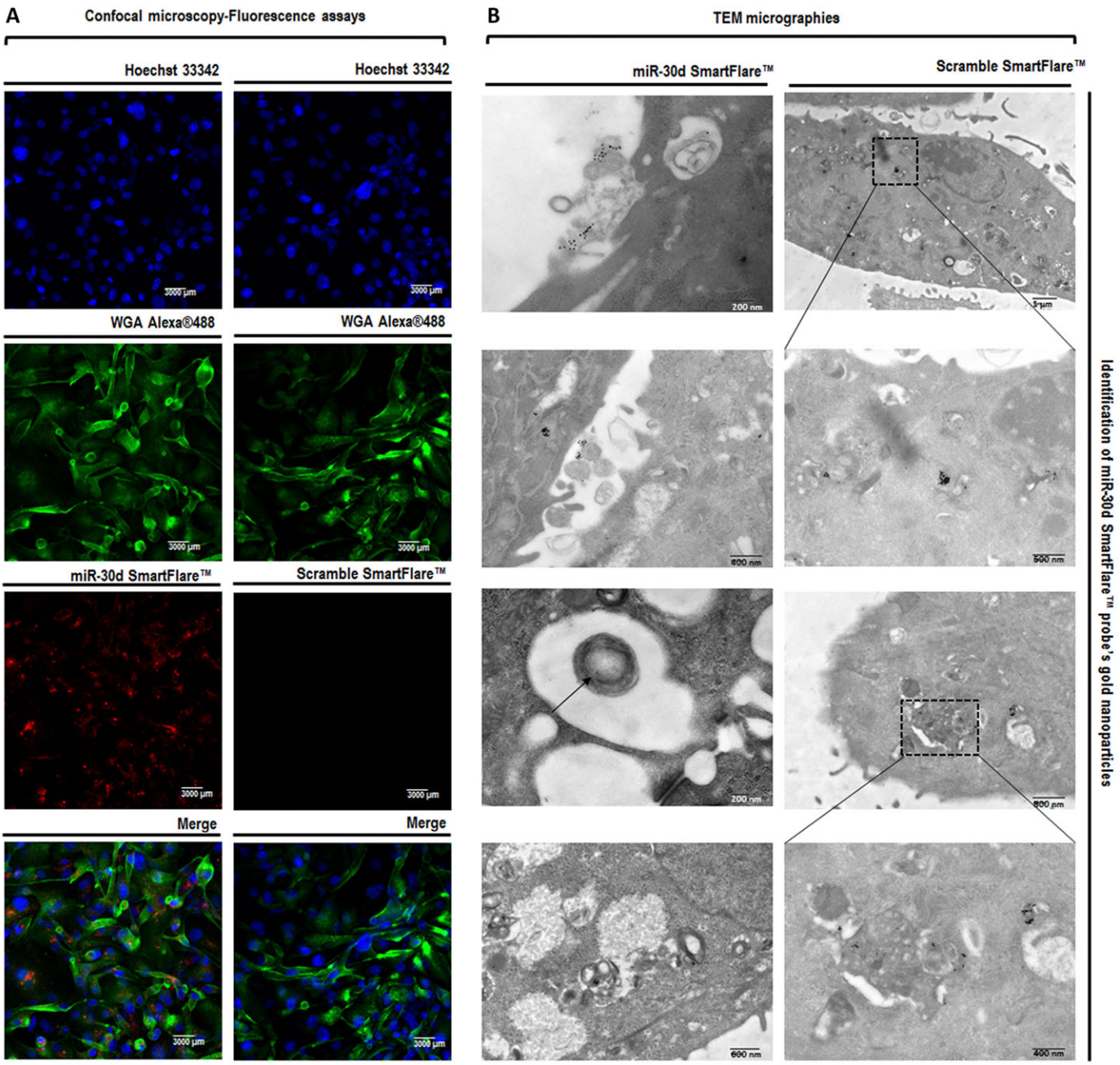

Fig. 3. *In vitro* identification of miR-30d production by hEECs. (A) Confocal microscopy images showing *in vitro* identification of miR-30d production by the human luminal epithelium. The first column shows the information obtained with a SmartFlare probe that specifically recognizes the presence of miR-30d in cells (labeled in red). Each probe consists of a gold nanoparticle conjugated to many copies of the same double-stranded oligonucleotide encoding the target sequence. One strand of the oligonucleotide bears a fluorophore (Cy3) that is quenched by its proximity to the gold core. When the nanoparticle contacts its target, the target RNA displaces the fluorophore. The reporter strand, now unquenched, fluoresces and can be detected using any fluorescence detection platform. The second column shows the images acquired with the control provided by the company (Millipore; Scramble SmartFlare probe). In this case, the capture strand is a scrambled sequence that does not recognize any target in cells and can therefore be used as a background control. In both cases, cell membranes appear to be labeled with WGA-Alexa 488 (green). (B) Transmission electron micrographs showing the location of the gold nanoparticles from the SmartFlare probes. The first column refers to the miR-30d SmartFlare probe, whereas the second column marks the location of the scramble probe within cells. The gold nanoparticles appear preferably located within multivesicular bodies and exosomes, thus suggesting that part of the miR-30d produced in cells can be found inside these membrane-bound organelles.

endometrial epithelium compared with that of scramble miRNA; this adhesive phenotype was significantly reduced when a specific miR-30d inhibitor blocking endogenous miR-30d was used (53.44±6.4% versus 18.55±3.72%, P=0.004; Fig. 6C). To analyze this effect in a homologous human model, a co-culture of a choriocarcinoma human cell line (JEG3, extravillous trophoblast used for its invasive phenotype) on top of hEECs was conducted for 24 h under three conditions: control without miRNA, in the presence of mimic miR-30d or in the presence of miR-30d inhibitor, in media previously conditioned for 72 h (n=15 spheroids per condition in each experiment). Analysis indicated there were no significant differences (P>0.05) in adhesion among the three conditions tested.

Development (2015) 142, 3210-3221 doi:10.1242/dev.124289

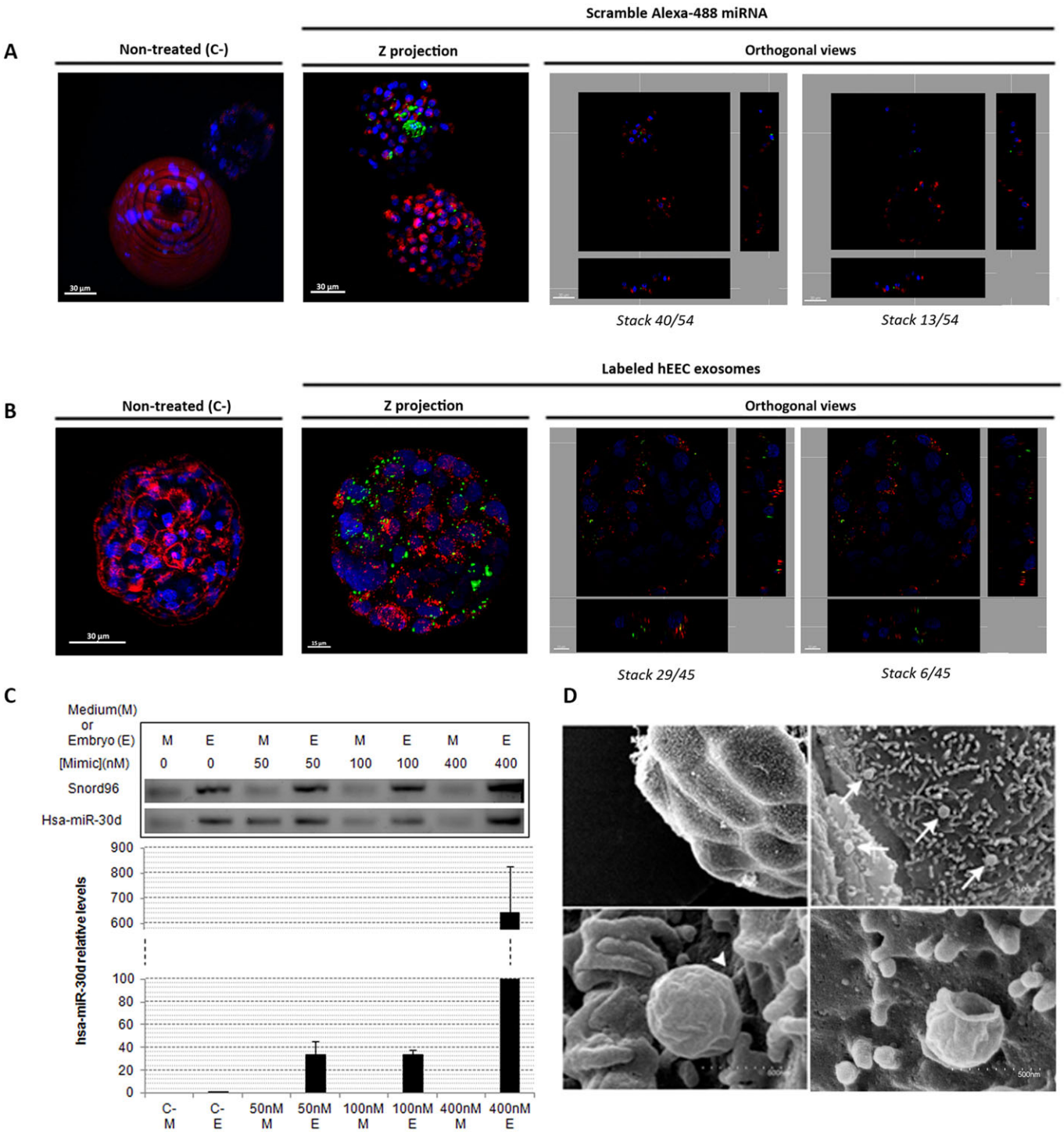

Fig. 4. Study of the ability of mouse embryos to take up free and exosome-associated miRNAs from the EF. (A) Confocal fluorescence microscopy of a live, hatching mouse blastocyst treated with 400 nM Alexa 488-scramble (green) miRNA for 72 h. Orthogonal sections performed with Imaris software confirm the internalization of free miRNAs inside embryos, discounting the possibility that these miRNAs could be adhered to the trophectoderm membrane (labeled in red). (B) Confocal microscopy images of a hatched blastocyst cultured with hEEC exosomes labeled with Vybrant DiO (green) for 24 h. Orthogonal sections performed with Imaris software confirm the internalization of exosomes inside embryos, discarding the possibility that these vesicles could be adhered to the trophectoderm membrane (labeled in red). (C) qPCR of embryos (E) treated with 0, 50, 100 or 400 nM mimic miR-30d (M). Gel bands, indicating the absence of Snord96 (housekeeping) or hsa-miR-30d in the final wash medium, are shown. (D) SEM images of a hatched mouse blastocyst with typical rounded vesicles (similar to exosomes) adhering to the trophectoderm. Arrows indicate vesicles adhering to the trophectoderm surface, arrowhead indicates a contact zone.

DISCUSSION

The 'Barker hypothesis' suggests that "the womb may be more important than the home", emphasizing the concept that the maternal endometrium has a reprogramming effect on the embryo, fetus and adult (Barker, 1990, 1997). To date, no strong evidence has implicated molecules secreted in the EF in the origin of adult diseases. However, accumulated evidence suggests that intrauterine exposure of fetuses in patients with diabetes or obesity confers an

Development (2015) 142, 3210-3221 doi:10.1242/dev.124289

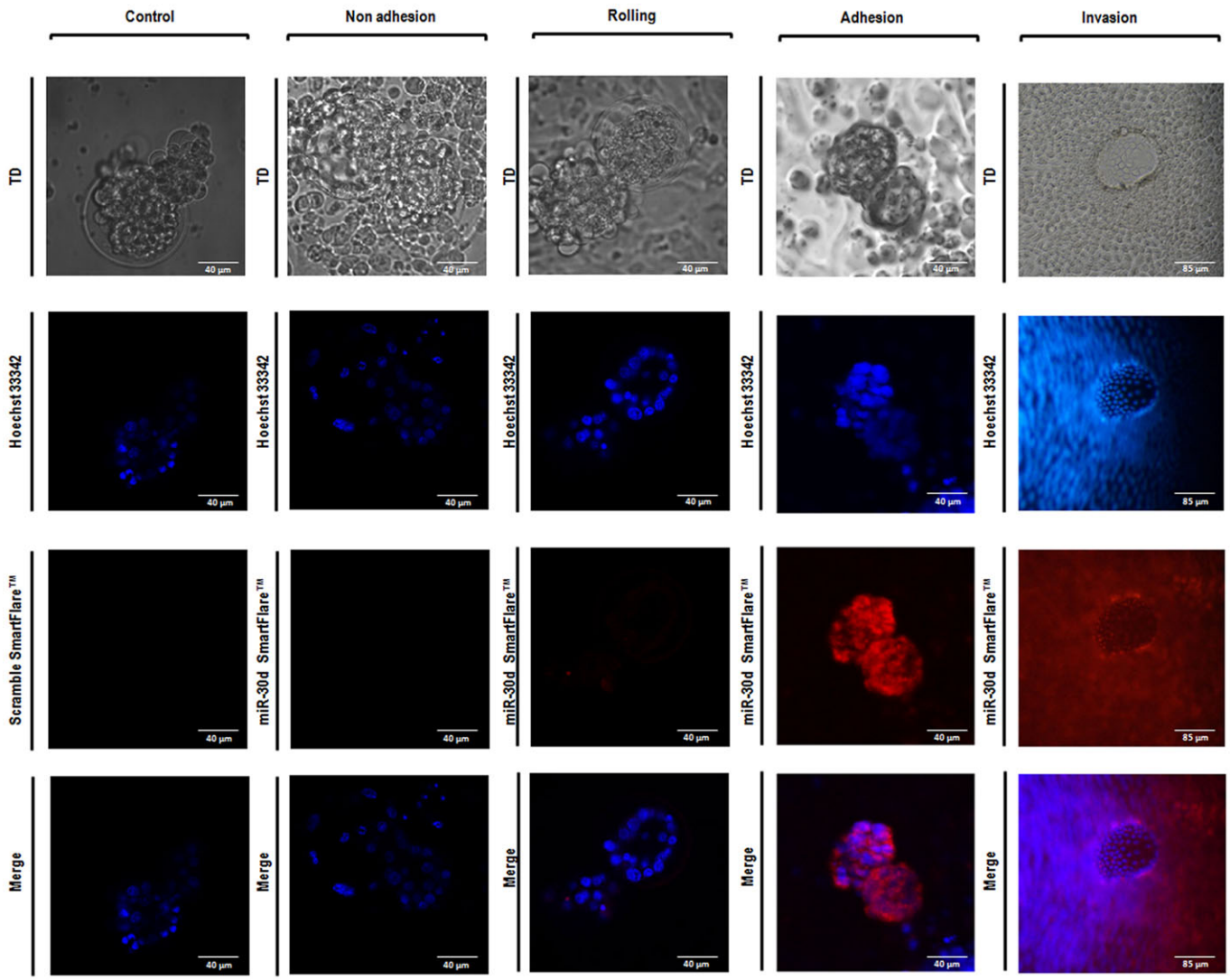

Fig. 5. *In vitro* identification of hsa-miR-30d uptake from hEECs by mouse embryos. Confocal microscopy images show the projection in the *z*-plane of mouse embryos that are specifically acquiring hsa-miR-30d (red) from SmartFlare-labeled-human epithelium. Micrographs are obtained in different moments of the co-culture, so the distinct stages of the implantation procedure could be identified. The intensity of the red signal progressively increases as implantation occurs. This phenomenon suggests that a direct cell-to-cell contact would probably be necessary for the transfer of hsa-miR-30d. This would explain why, in the adhesion stage, in which the contact is complete, the Cy3 label is distributed throughout the embryo, whereas just those cells of the trophectoderm directly polarized towards the epithelium are marked in the rolling stage.

increased risk of these diseases in the adult life of offspring (Clausen et al., 2008). Similarly, follow-up studies of the Pima Native American community in Arizona, a population with an extremely high prevalence of type-2 diabetes (T2D) and obesity, demonstrate that the offspring of mothers affected by T2D during pregnancy were at substantially higher risks of developing both T2D (45% versus 1.4%) and obesity (58% versus 17%) than children born to the same mother in a non-diabetic status (Dabelea et al., 2000).

Our study, which is consistent with other evidence (Ng et al., 2013), demonstrates the presence of miRNAs differentially secreted in human EF throughout the menstrual cycle. In this study, hsa-miR-30d was the most differentially expressed miRNA during the WOI; miR-30d was previously described in endometrial physiology (Moreno-Moya et al., 2014). Therefore, we used this molecule as the paradigm for our hypothesis regarding maternal transcriptomic reprogramming of the pre-implantation embryo. Hsa-miR-30d belongs to the miR-30 family comprising six molecules (hsa-miR-30a-f) that possess a sequence highly conserved between species. In general, the miR-30 family is ubiquitously expressed in humans and has been associated with several functions in different cell types. For example, this family participates in the epithelial-to-mesenchymal transition (Özcan, 2014), confers an epithelial phenotype to human pancreatic cells (Joglekar et al., 2014), regulates apoptosis through TP53 targeting and the mitochondrial fusion machinery (Li et al., 2010), and participates in ectoderm differentiation during embryonic development by targeting the embryonic ectoderm development (EED) protein (Song et al., 2011).

MiRNAs are often transported through exosomes, which are emerging as important mediators of intercellular communication. The secretion of exosomes from the apical surface of endometrial glands was confirmed here by electron microscopy, which is consistent with the existence of endosomes in epithelial cells and small vesicles in EF observed by immunohistochemistry. Further, primary hEECs were found to actively secrete large quantities of

Development (2015) 142, 3210-3221 doi:10.1242/dev.124289

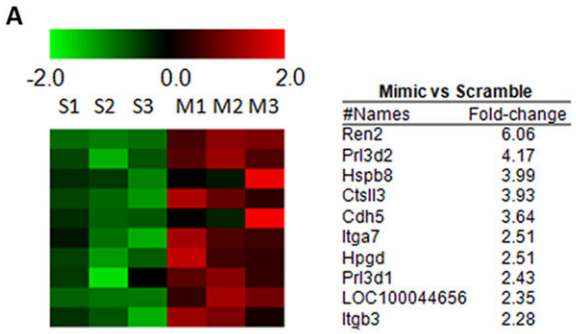

Mimic vs Scramble

#Names	Fold-change
Ren2	6.06
Prl3d2	4.17
Hspb8	3.99
Ctsll3	3.93
Cdh5	3.64
Itga7	2.51
Hpgd	2.51
Prl3d1	2.43
LOC100044656	2.35
Itgb3	2.28

B

Biological process	p-value	Genes
cell adhesion	0.02	ITGA7, ITGB3, CDH5
biological adhesion	0.02	ITGA7, ITGB3, CDH5
integrin-mediated signaling pathway	0.03	ITGA7, ITGB3
developmental maturation	0.04	REN2, LOC100044656, CDH5

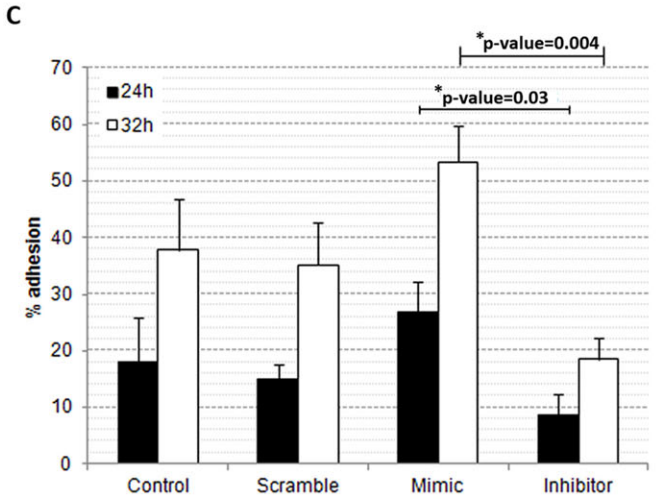

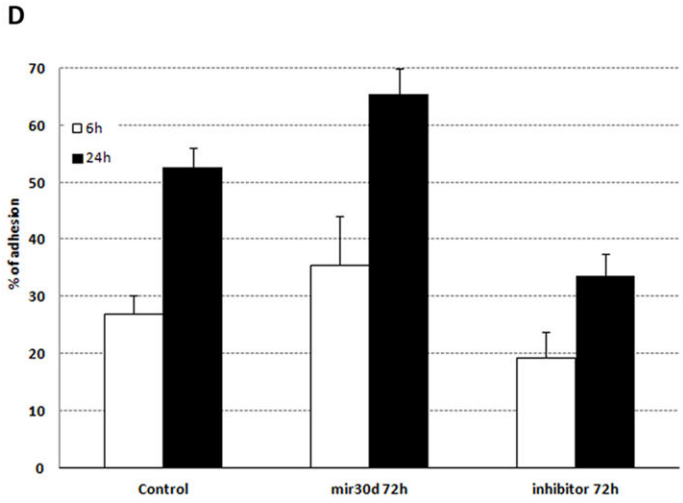

Fig. 6. Transcriptional and functional modifications in mouse embryos induced by hsa-miR-30d. (A) Supervised and standardized heat map of differentially expressed genes obtained from gene expression microarrays in embryos treated with scramble miRNA (S) or mimic miR-30d (M). (B) Significantly affected biological processes based on predictions made by the web-based tool DAVID. (C) Mouse blastocyst adhesion assay showing a functional effect related to miR-30d uptake. (D) JEG3 adhesion assay showing a functional effect related to miR-30d uptake. (C,D) Data are expressed as mean±s.e.m.

exosomes into the conditioned media, and labeling experiments with miR30-d revealed that this miRNA is internalized in vesicles and secreted in exosomes. In addition, miR-30d was detected in the remaining supernatant from EF and conditioned media samples after harvesting of exosomes by ultracentrifugation, suggesting that other soluble forms are also present in the EF. Several tracking experiments showed that exosomes loaded with miR-30d were secreted from hEECs and could be internalized by trophoblastic cells of murine embryos adhered to hEECs. These findings demonstrate that the maternal factors can be transmitted through EF to the embryo.

Several mechanisms, such as endocytosis or fusion of the exosomes with the plasma membrane (Colombo et al., 2014), have been proposed to explain how exosome content is released into target cells. Here, the addition of free miRNAs into culture media at different concentrations resulted in the incorporation of these molecules into the hatched trophoblastic cells. In electron microscopy images, we observed that murine embryos presented microvilli and what appeared to be small pores interspaced along the trophoblastic surface. This finding could explain how blastocysts mediate a fast exchange of nutrients and molecules.

To understand the functional role of maternal miR-30d incorporation into the embryo, transcriptomic studies were performed to compare the effects of mimic miR-30d miRNAs and scramble miRNA in murine embryos. Expression arrays demonstrated that embryos treated with miR-30d exhibited increased expression of ten genes, including those encoding adhesion molecules such as ITGB3, ITGA7 and CDH5. The induction of this adhesive phenotype was validated *in vitro* by adhesion assays showing a significant increase in the adhesion of murine embryos treated with miR-30d mimic versus miR-30d inhibitor. To clarify whether these findings could be extrapolated to humans, an *in silico* analysis of the putative targets of miR-30d in mice and humans was performed using the TargetScan database (http://www.targetscan.org). Specifically, 1594 targets were identified in humans and 1396 in mice, with 1108 common targets between both species (supplementary material Table S8). As most of the target genes coincided, we expected that the physiological functions in which they were involved could be similar. The gene ontology (GO) terms associated with these genes were analyzed using the Ensembl database (http://www.ensembl.org/), identifying a total of 2422 common terms between humans and mice (supplementary material Tables S9, S10). Notably, among the common terms, 19 were involved in embryonic development, highlighting the relevance of this paradigm.

In summary, we have identified a novel cell-to-cell communication mechanism that involves the delivery of endometrial miRNAs from the maternal endometrium to the pre-implantation embryo. Exosome-associated and free hsa-miR-30d was taken up by the embryo from the EF. Trophectoderm cells are able to take up maternal miRNAs; these miRNAs are proposed to be incorporated into the RISC complex to exert gene regulation under physiological conditions, thereby resulting in the observed modifications to the transcriptome and embryo adhesion (Fig. 7).

Development (2015) 142, 3210-3221 doi:10.1242/dev.124289

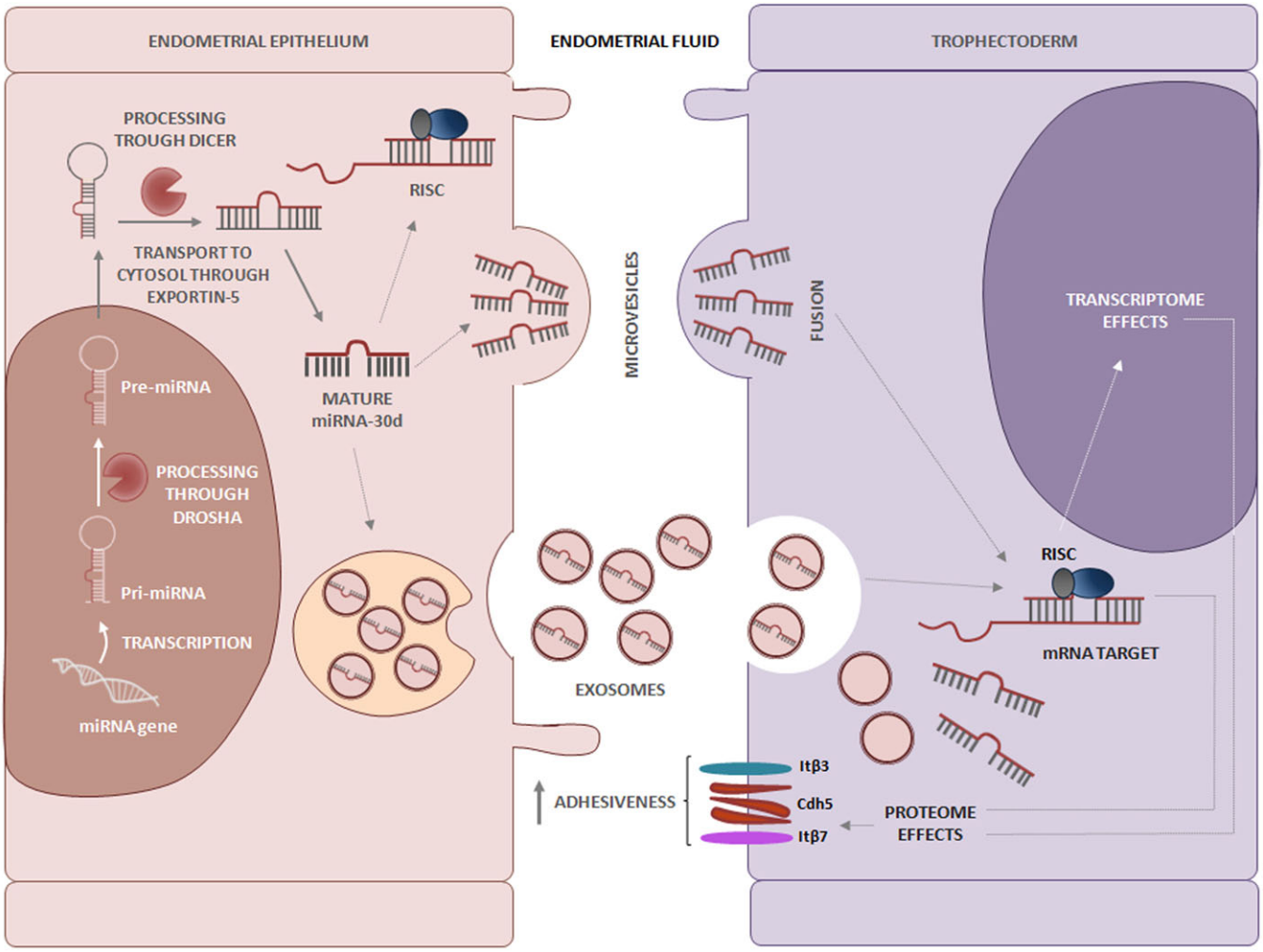

Fig. 7. Schematic of a novel maternal-fetal cross-talk mechanism promoted by hsa-miR-30d. Hsa-miR-30d is delivered to the EF from the maternal endometrium, modifying the embryo transcriptome and its adhesive phenotype.

MATERIALS AND METHODS

EF samples

This study was approved by the institutional review board of the Instituto Valenciano de Infertilidad (IVI) (project number 1204-C-102-FV-F), Valencia, Spain. Written informed consent was obtained from all donors involved in this prospective study. Healthy participants with regular menstrual cycles of 25-33 days and without underlying endometrial pathologies were selected for collection of EF samples (n=20). None of the women received hormonal treatment in the 3 months preceding biopsy and EF collection. Women were divided into five groups (n=4 per group), according to the stage of the cycle when the samples were obtained (EP, LP, ES, LS and WOI), based on the date of the last menstruation (supplementary material Table S1). Briefly, a speculum was inserted into the subject while in the lithotomy position. Next, the cervix was cleansed and a flexible catheter (Wallace; Smiths Medical) gently introduced to aspirate 20-50 µl of endometrial secretion. EF samples were preserved at −80°C until they were used for RNA extraction.

RNA extraction from EF

RNA extraction was performed using the miRNeasy Kit (Qiagen) and quantified using a NanoDrop spectrophotometer (Thermo Fisher Scientific). To characterize the fraction of miRNAs present, a Small RNA kit and a Small RNA assay were used on samples with the Agilent 2100 Bioanalyzer (Agilent Technologies). MiRNA microarray analysis was performed in triplicate. miRNAs were quantified using the Small RNA LabChip BioAnalyzer 2100 (Agilent Technologies) (see supplementary material Table S1A and Fig. S1).

miRNA microarray analysis

The grouped EF cohorts were analyzed using human miRNA v3.0 8×15 K microarrays (Agilent Technologies), which evaluate the expression of 866 human miRNAs. Total RNA was processed from each sample according to the manufacturer's instructions and then scanned. Data obtained for each probe were normalized and $\log_2$-transformed using R software and Bioconductor database libraries. The web-based Babelomics tool (Medina et al., 2010) was used for merging the resulting data matrix in accordance with the mean number of replicates for each probe. Next, the data matrix was analyzed, and differentially expressed miRNAs were listed together with their fold change. PCA of the differentially expressed miRNAs was performed using Babelomics. IPA software (Ingenuity Systems) was used for predicting the affected biological functions and any previously reported interactions between the miRNAs and target genes. Raw data are available in the Gene Expression Omnibus (GEO) database under the accession number GSE44558.

miRNA PCR validation

To confirm the results of the miRNA microarrays, hsa-miR-30d was selected due to its significantly higher expression during the WOI. Absolute qPCR was performed using the miScript reverse transcription and miScript SYBR Green PCR kits (Qiagen). hsa-miR-30d concentration was estimated using a standard curve ranging from 20 fM to 2 mM.

Development (2015) 142, 3210-3221 doi:10.1242/dev.124289

Immunohistochemistry

Formalin-fixed and paraffin-embedded human endometrial biopsies were sectioned and mounted on glass slides coated with IHC (DAKO) as described previously (Dominguez et al., 2010). The primary antibody was mouse monoclonal anti-CD63 (Abcam), which was incubated overnight. Secondary antibodies were included in the LSAB Peroxidase Kit (DAKO) and were valid against mouse-origin primary antibodies.

Isolation of exosomes from EF

EF samples were diluted in PBS (Life Technologies), vortexed vigorously and filtered using a 0.22-µm syringe filter (Pall). The filtrates were centrifuged at 300 ***g*** for 10 min to remove whole cells. The supernatant was subjected to a second centrifugation at 2000 ***g*** for 10 min to remove dead cells, then centrifuged again at 10,000 ***g*** for 30 min to remove cell debris. The supernatants were re-filtered with a 0.22-µm syringe filter (Pall) and ultracentrifuged at 120,000 ***g*** for 70 min. Pellets containing exosomes were used for electron microscopy, embryo uptake assays, RNA extraction and qPCR.

hEEC cultures and exosome isolation

Endometrial biopsy samples obtained from healthy donors were processed to separate the epithelial and stromal cell fractions by collagenase digestion as described previously (Simón et al., 1997), and the purified hECCs were plated into 24-well plates (Falcon; Becton Dickinson). When cultures reached confluence, they were washed with DMEM (Sigma-Aldrich) to remove FBS-contaminated exosomes and cultured in DMEM (Sigma-Aldrich). After 48 h, the conditioned medium was collected and exosomes were isolated as described in the section above.

Western blotting

Antibodies against human CD63, CD9, CD81 (System Biosciences) and calnexin (Enzo Life Sciences) were used for western blotting. Isolated exosomes secreted from primary hEEC cultures were lysed in RIPA buffer at 4°C for 20 min. Samples were quantified using a BCA protein assay kit (Pierce) and separated by SDS-PAGE before electro-transfer to PVDF membranes (Bio-Rad). Membranes were incubated overnight with specific primary antibodies diluted 1:1000 in 5% BSA. Next, membranes were washed three times with PBS-T 1% and incubated with secondary anti-mouse and anti-rabbit antibodies (System Biosciences) at a concentration of 1:20,000. Finally, target proteins were detected by using the SuperSignal West Femto Chemiluminiscent kit (Thermo Fisher Scientific).

RNase treatment of exosomes

To test whether miRNAs contained in exosomes were protected from degradation, total RNA extraction was performed on isolated exosomes using the miRNeasy Kit (Qiagen). Extracted RNA was treated with 10 ng/µl of RNase A (Sigma-Aldrich) at room temperature for 30 min. RNA was quantified using a NanoDrop spectrophotometer (Thermo Fisher Scientific) and the miRNA fraction evaluated using a Small RNA kit and a Small RNA assay on an Agilent 2100 Bioanalyzer (supplementary material Table S1 and Fig. S1).

In vitro identification of miR-30d production by hEECs

Confluent hEECs were incubated for 20 h with 8 µl of a work solution comprised of a SmartFlare probe (miR-30d probe or scramble control) (Millipore) and PBS in a proportion of 1:20. After labeling was completed, cells were incubated with 5 µg/ml Hoechst 33342 (Sigma-Aldrich) and WGA Alexa 488 (Life Technologies, Molecular Probes). Next, hEECs were washed three times with medium and visualized with a 60× water immersion confocal microscope (FV1000, Olympus). When the confocal assay was finished, cells were used in a TEM study to identify the location of the gold nanoparticles from the SmartFlare probes.

Recovery of pre-implantation mouse embryos

The $B6C3F_1$ mouse strain was purchased from Charles River Laboratories. Female mice, ages 6-8 weeks, were primed to ovulate by administering 10 IU of pregnant mare serum gonadotropin (Sigma-Aldrich). Then, 48 h later, 10 IU of human chorionic gonadotropin (Sigma-Aldrich) were administrated. Females were housed overnight with male studs and examined the following morning for the presence of a vaginal plug (classified as day 1 of pregnancy). On day 1.5 of pregnancy, the mice were euthanized by cervical dislocation and embryos were flushed from the oviduct with PBS (Life Technologies) using a 30-gauge blunt needle (code procedure 2015/VSC/PEA/00048). Embryos were then washed four times in fresh CCM-30 (Qiagen) medium and used for transcriptomic assays, electron microscopy, confocal microscopy and adhesion assays. Studies were carried out using protocols (Garrido-Gomez et al, 2012; 2014/VSC/PEA/00119 tipo2 and 2015/VSC/PEA/00048) approved by the Ministry of Presidency, Agriculture, Fisheries, Food and Water, Valencia (Spain) and the Animal Care and Use Committee of the Valencia University.

Free miRNA uptake by embryo

Before studying the internalization of free miRNAs by confocal microscopy, an *in vitro* time course to select the most suitable concentration of hsa-miR-30d was performed. For this, day-1.5 mouse embryos were cultured for 72 h with 50, 100 and 400 nM mimic hsa-miR-30d and Alexa 488 scramble miRNA. To validate the success of the internalization process, a qPCR was performed in both control and hsa-miR-30d-treated embryos. miRNA extraction was performed with Arcturus PicoPure RNA Isolation Kit (Life Technologies). Once the working concentration (400 nM) was selected, confocal microscopy assays were performed.

Exosome staining and embryo co-culture

Previously isolated exosomes were incubated with 5 µM fluorescent Vybrant DiO (Life Technologies) at 37°C for 30 min. After labeling, exosomes were collected and ultracentrifuged to wash off the excess dye, added to hatching embryos and incubated for 12-24 h.

Confocal fluorescence microscopy

For visual inspection of the uptake of free miRNA and exosomes by mouse embryos, the aforementioned samples were incubated at 37°C for 30 min with 5 µg/ml of Hoechst 33342 (Sigma-Aldrich) and 10 µg/ml of WGA-Texas Red (Life Technologies, Molecular Probes) for nuclear and membrane staining, respectively. Next, excess dye was removed by transferring the embryos to new wells covered with fresh medium. Finally, embryos were placed in an 8-well µ-Slide chamber (Ibidi) filled with PBS and visualized with a 60× water immersion confocal microscope (FV1000, Olympus). Data analysis renderings and live animations were carried out using Imaris software (Oxford Instruments).

Electron microscopy

To assess the presence of exosomes in primary hEECs, cells and isolated exosomes were fixed in Karnovsky's solution (Doughty et al., 1997). After incubation with isolated exosomes, pre-implantation mouse embryos were fixed for 2-24 h. Briefly, freshly isolated primary hEECs were post-fixed in osmium tetroxide, washed and stained with uranyl acetate. Samples were dehydrated, embedded in epoxy resin, ultrasectioned, transferred to carbon-coated grids, and observed using a JEM-1010 transmission electron microscope (Jeol Korea) at 100 kV. Pre-implantation mouse embryos were processed for TEM in the same way but were embedded in agarose before post-fixation. Exosomes were re-suspended in 50 µl of Karnovsky's solution, incubated for 1 h on a Formvar carbon-coated grid and contrasted with uranyl acetate. For SEM, post-fixed embryos were subjected to critical point dehydration and observed in an S-4100 scanning electron microscope (Hitachi) at 10 kV.

In vitro identification of miR-30d uptake by mouse embryos

Day-1.5 mouse embryos were incubated with hEEC previously labeled with the SmartFlare probe (miR-30d probe or scramble control) (Millipore). Before the co-culture took place, medium was removed from the cells to ensure that the signal transferred to the embryos came from the hEEC. After 30 h of co-culture, 5 µg/ml of Hoechst 33342 (Sigma-Aldrich) was added, and analysis was performed with a 60× water immersion confocal microscope (FV1000, Olympus).

Development (2015) 142, 3210-3221 doi:10.1242/dev.124289

Transcriptomic microarray analyses

A total of 360 mouse embryos from day 1.5 (30 per condition, four conditions, including the untreated, all conditions in triplicate) were treated with either 400 nM of scramble miRNA or mimic or inhibitor of miR-30d for 72 h; we performed three biological triplicates, and the total number of mouse embryos used was 1080. Next, embryos were analyzed using Agilent GE 4×44 K Mouse v3 microarrays. Total RNA from each sample was processed according to the manufacturer's instructions. After scanning, microarray data were preprocessed and normalized using the R/Bioconductor package *limma*. Quantile normalization was applied to standardize probe intensities across samples. Differential gene expression was assessed using the *RankProd* library of Bioconductor (http://bioconductor.org). The *RankProd* methodology uses a non-parametric statistic to estimate differential expression for each gene and a permutation scheme to estimate *P*-values and control for the FDR. Log fold changes created by *RankProd* were used to rank miRNAs according to the mean expression differences between groups. Microarray results were validated by qPCR as previously described (Estella et al., 2012b) using two of the most significantly upregulated genes, *Cdh5* and *Itgb3* (supplementary material Fig. S3 and Table S1B).

Embryo adhesion assay

Epithelial endometrial cells from six donors were cultured until confluence, and 15 embryos per condition (total of four conditions) were added in three independent experiments (i.e. 360 embryos). Mouse blastocysts expanded with normal morphology were cultured in the presence of 400 nM mimic miR-30d, Alexa 488-scramble miRNA or miR-30d inhibitor (Qiagen) for 72 h. The attachment of mouse blastocysts to the epithelial cell monolayer was measured after 24 and 32 h by mechanical assay. Briefly, plates were moved on a rotation shaker for 10 s, and floating blastocysts were deemed to be unattached.

JEG3 adhesion assay

JEG3 cells, a human choriocarcinoma cell line used as a model to simulate primary trophoblast cells, were grown in a monolayer with Eagle's Minimal Essential Medium (EMEM; PPA) supplemented with 10% FBS, 0.1% fungizone and 0.1% gentamicin until 80% confluence. JEG3 cells were cultured in the presence of 400 nM miR-30 mimic, Alexa 488-scramble miRNA or miR-30d inhibitor (Qiagen) for 72 h and then plated in an ultra-low-attachment plate for spheroid formation with the same culture medium. Spheroids were observed after 24 h. hEECs from three donors were cultured until confluence and 15 spheroids added per condition. Adhesion was analyzed after 6 and 24 h by mechanical assays. After a brief rotation on the shaker, floating spheroids were considered to be unattached.

Statistical analysis

For miRNA microarrays of EF, the pre-processed (log-transformed, normalized and merged based on the number of probe replicates) data matrix was introduced into an SAM module in the MeV statistical analysis software. Samples were grouped into EP, LP, ES, WOI and LS phases and each group analyzed relative to the WOI group using an FDR correction of <5%. The fold changes in miRNA among the various samples and groups were calculated. For embryo gene expression microarrays, the pre-processed data matrix was introduced into a *Rank Product* module in MeV. Samples were assigned to their respective categories based on the intended comparison. Median differences among conditions in embryo adhesion experiments were evaluated using the Kruskal–Wallis test, after confirming that data did not follow a normal distribution. A one-way ANOVA was applied for the analysis of JEG3 adhesion assays. In both cases, Statgraphics Centurion software package (v.16.1.11) was used. *P*-values <0.05 were considered significant.

In silico analysis of transcriptomic effects

To explore how the transcriptomic effects caused by hsa-miR-30d in mouse could relate to human, the TargetScan database was used to find potential targets of miR-30d in both species. Once these were established, the Ensembl website (http://www.ensembl.org/) was used to determine which GO terms were associated with the output of targets obtained. With all the information available, a screening of the coincidences existing between the two species was conducted.

Acknowledgements

We thank Prof. Eulogio Valentin for helping with the exosome separation protocol. We also thank David Montaner from Genometra Company for his excellent work on the microarrays analysis and helping us with the statistical methodology. We thank Blanca Simon and Inmaculada Moreno, PhD, for help in reading and correcting the manuscript. We thank Sheila M. Cherry, PhD, ELS, President and Senior Editor from Fresh Eyes Editing, LLC for her excellent work editing this manuscript. Finally, we are grateful to the Electronic Microscopy Service (SCSIE) at the University of Valencia for their help.

Competing interests

The authors declare no competing or financial interests.

Author contributions

F.V.: conception and design, collection and assembly of data, data analysis and interpretation, manuscript writing, final approval of manuscript and fundraising; J.M.M.-M.: conception and design, collection and assembly of data, data analysis and interpretation, and final approval of manuscript; N.B.: collection and assembly of data, data analysis and interpretation, manuscript writing and final approval of manuscript; A.G.: collection and assembly of data and final approval of manuscript; M.H.: collection and assembly of data and final approval of manuscript; S.M.: collection and assembly of data and final approval of manuscript; A.M.: data analysis and interpretation and final approval of manuscript; C.S.: conception and design, data analysis and interpretation, manuscript writing, final approval of manuscript and fundraising.

Funding

This work was supported by the IVI Foundation and Miguel Servet Program Type I of Instituto de Salud Carlos III [CP13/00038]; FIS project [PI14/00545] and Fondos Feder to F.V.; and the 'Atracció de Talent' Program from VLC-CAMPUS [UV-INV-PREDOC14-178329 to N.B.].

Supplementary material

Supplementary material available online at
http://dev.biologists.org/lookup/suppl/doi:10.1242/dev.124289/-/DC1

References

Altmäe, S., Martínez-Conejero, J. A., Salumets, A., Simón, C., Horcajadas, J. A. and Stavreus-Evers, A. (2010). Endometrial gene expression analysis at the time of embryo implantation in women with unexplained infertility. *Mol. Hum. Reprod.* **16**, 178-187.

Ambros, V. and Chen, X. (2007). The regulation of genes and genomes by small RNAs. *Development* **134**, 1635-1641.

Barker, D. J. (1990). The fetal and infant origins of adult disease. *BMJ* **301**, 1111.

Barker, D. J. P. (1997). The long-term outcome of retarded fetal growth. *Clin. Obstet. Gynecol.* **40**, 853-863.

Bartel, D. P. (2004). MicroRNAs: genomics, biogenesis, mechanism, and function. *Cell* **116**, 281-297.

Boomsma, C. M., Kavelaars, A., Eijkemans, M. J. C., Amarouchi, K., Teklenburg, G., Gutknecht, D., Fauser, B. J. C. M., Heijnen, C. J. and Macklon, N. S. (2009). Cytokine profiling in endometrial secretions: a non-invasive window on endometrial receptivity. *Reprod. Biomed. Online* **18**, 85-94.

Burton, G. J., Jauniaux, E. and Charnock-Jones, D. S. (2007). Human early placental development: potential roles of the endometrial glands. *Placenta* **28**, S64-S69.

Caballero-Campo, P., Dominguez, F., Coloma, J., Meseguer, M., Remohí, J., Pellicer, A. and Simón, C. (2002). Hormonal and embryonic regulation of chemokines IL-8, MCP-1 and RANTES in the human endometrium during the window of implantation. *Mol. Hum. Reprod.* **8**, 375-384.

Cervero, A., Horcajadas, J. A., MartÍn, J., Pellicer, A. and Simón, C. (2004). The leptin system during human endometrial receptivity and preimplantation development. *J. Clin. Endocrinol. Metab.* **89**, 2442-2451.

Cha, J., Sun, X. and Dey, S. K. (2012). Mechanisms of implantation: strategies for successful pregnancy. *Nat. Med.* **18**, 1754-1767.

Cha, J., Vilella, F., Dey, S. K. and Simón, C. (2013). Molecular interplay in successful implantation. *Science* Ten critical Topics in Reproductive Medicine, 44-48.

Chen, K., Chen, X., He, J., Ding, Y., Geng, Y., Liu, S., Liu, X. and Wang, Y. (2015). Mouse endometrium temporal and spatial expression mrna and microrna associated with embryo implantation. *Reprod. Sci.*

Clausen, T. D., Mathiesen, E. R., Hansen, T., Pedersen, O., Jensen, D. M., Lauenborg, J. Damm, P. (2008). High Prevalence of Type 2 Diabetes and

Pre-Diabetes in Adult Offspring of Women With Gestational Diabetes Mellitus or Type 1 Diabetes.
Colombo, M., Raposo, G. and Théry, C. (2014). Biogenesis, secretion, and intercellular interactions of exosomes and other extracellular vesicles. *Annu. Rev. Cell Dev. Biol.* **30**, 255-289.
Cross, J. C., Werb, Z. and Fisher, S. J. (1994). Implantation and the placenta: key pieces of the development puzzle. *Science* **266**, 1508-1518.
Dabelea, D., Hanson, R. L., Lindsay, R. S., Pettitt, D. J., Imperatore, G., Gabir, M. M., Roumain, J., Bennett, P. H. and Knowler, W. C. (2000). Intrauterine exposure to diabetes conveys risks for type 2 diabetes and obesity: a study of discordant sibships. *Diabetes* **49**, 2208-2211.
De los Santos, M. J., Mercader, A., Francés, A., Portolés, E., Remohí, J., Pellicer, A. and Simón, C. (1996). Role of endometrial factors in regulating secretion of components of the immunoreactive human embryonic interleukin-1 system during embryonic development. *Biol. Reprod.* **54**, 563-574.
Domínguez, F., Garrido-Gómez, T., López, J. A., Camafeita, E., Quiñonero, A., Pellicer, A. and Simón, C. (2009). Proteomic analysis of the human receptive versus non-receptive endometrium using differential in-gel electrophoresis and MALDI-MS unveils stathmin 1 and annexin A2 as differentially regulated. *Hum. Reprod.* **24**, 2607-2617.
Dominguez, F., Simón, C., Quiñonero, A., Ramírez, M. Á., González-Muñoz, E., Burghardt, H., Cervero, A., Martínez, S., Pellicer, A., Palacín, M. et al. (2010). Human endometrial CD98 is essential for blastocyst adhesion. *PLoS ONE* **5**, e13380.
Doughty, M. J., Bergmanson, J. P. and Blocker, Y. (1997). Shrinkage and distortion of the rabbit corneal endothelial cell mosaic caused by a high osmolality glutaraldehyde-formaldehyde fixative compared to glutaraldehyde. *Tissue Cell* **29**, 533-547.
Estella, C., Herrer, I., Atkinson, S. P., Quiñonero, A., Martínez, S., Pellicer, A. and Simón, C. (2012a). Inhibition of histone deacetylase activity in human endometrial stromal cells promotes extracellular matrix remodelling and limits embryo invasion. *PLoS ONE* **7**, e30508.
Estella, C., Herrer, I., Moreno-Moya, J. M., Quiñonero, A., Martínez, S., Pellicer, A. and Simón, C. (2012b). miRNA signature and Dicer requirement during human endometrial stromal decidualization in vitro. *PLoS ONE* **7**, e41080.
Garrido-Gómez, T., Dominguez, F., Quiñonero, A., Estella, C., Vilella, F., Pellicer, A. and Simón, C. (2012). Annexin A2 is critical for embryo adhesiveness to the human endometrium by RhoA activation through F-actin regulation. *FASEB J.* **26**, 3715-3727.
Godfrey, K. M. and Barker, D. J. P. (2001). Fetal programming and adult health. *Public Health Nutr.* **4**, 611-624.
González, R. R., Caballero-Campo, P., Jasper, M., Mercader, A., Devoto, L., Pellicer, A. and Simón, C. (2000). Leptin and leptin receptor are expressed in the human endometrium and endometrial leptin secretion is regulated by the human blastocyst. *J. Clin. Endocrinol. Metab.* **85**, 4883-4888.
Hannan, N. J., Stephens, A. N., Rainczuk, A., Hincks, C., Rombauts, L. J. F. and Salamonsen, L. A. (2010). 2D-DiGE analysis of the human endometrial secretome reveals differences between receptive and nonreceptive states in fertile and infertile women. *J. Proteome Res.* **9**, 6256-6264.
Joglekar, M. V., Patil, D., Joglekar, V. M., Rao, G. V., Reddy, N. D., Mitnala, S., Shouche, Y. and Hardikar, A. (2014). The miR-30 family microRNAs confer epithelial phenotype to human pancreatic cells. *Islets* **1**, 137-147.
Kang, Y.-J., Lees, M., Matthews, L. C., Kimber, S. J., Forbes, K. and Aplin, J. D. (2015). MiR-145 suppresses embryo-epithelial juxtacrine communication at implantation by modulating maternal IGF1R. *J. Cell Sci.* **128**, 804-814.
Kennedy, A. R., Pissios, P., Otu, H., Xue, B., Asakura, K., Furukawa, N., Marino, F. E., Liu, F.-F., Kahn, B. B., Libermann, T. A., et al. (2007). A high-fat, ketogenic diet induces a unique metabolic state in mice. *Am. J. Physiol. Endocrinol. Metab.* **292**, E1724-E1739.
Khalil, A., Jauniaux, E., Cooper, D. and Harrington, K. (2009). Pulse Wave Analysis in Normal Pregnancy: A Prospective Longitudinal Study. *PLoS ONE* **4**, e6134.
Kuokkanen, S., Chen, B., Ojalvo, L., Benard, L., Santoro, N. and Pollard, J. W. (2010). Genomic profiling of microRNAs and messenger RNAs reveals hormonal regulation in microRNA expression in human endometrium. *Biol. Reprod.* **82**, 791-801.
Li, J., Donath, S., Li, Y., Qin, D., Prabhakar, B. S. and Li, P. (2010). miR-30 regulates mitochondrial fission through targeting p53 and the dynamin-related protein-1 pathway. *PLoS Genet.* **6**, e1000795.
Licht, P., Russu, V. and Wildt, L. (2001). On the role of human chorionic gonadotropin (hCG) in the embryo-endometrial microenvironment: implications for differentiation and implantation. *Semin. Reprod. Med.* **19**, 37-48.
Liu, X., Gao, R., Chen, X., Zhang, H., Zheng, A., Yang, D., Ding, Y., Wang, Y. and He, J. (2013). Possible roles of mmu-miR-141 in the endometrium of mice in early pregnancy following embryo implantation. *PLoS ONE* **8**, e67382.
Mansour, R., Ishihara, O., Adamson, G. D., Dyer, S., de Mouzon, J., Nygren, K.-G., Sullivan, E. and Zegers-Hochschild, F. (2014). International committee for monitoring assisted reproductive technologies world report: assisted reproductive technology 2006. *Hum. Reprod.* **29**, 1536-1551.
Martín, J. C., Jasper, M. J., Valbuena, D., Meseguer, M., Remohí, J., Pellicer, A. and Simón, C. (2000). Increased adhesiveness in cultured endometrial-derived cells is related to the absence of moesin expression. *Biol. Reprod.* **63**, 1370-1376.
Mascarenhas, M. N., Flaxman, S. R., Boerma, T., Vanderpoel, S. and Stevens, G. A. (2012). National, regional, and global trends in infertility prevalence since 1990: a systematic analysis of 277 health surveys. *PLoS Med.* **9**, e1001356.
Mathivanan, S., Fahner, C. J., Reid, G. E. and Simpson, R. J. (2011). ExoCarta 2012: database of exosomal proteins, RNA and lipids. *Nucleic Acids Res.* **40**, D1241-D1244.
Medina, I., Carbonell, J., Pulido, L., Madeira, S. C., Goetz, S., Conesa, A., Tárraga, J., Pascual-Montano, A., Nogales-Cadenas, R., Santoyo, J. et al. (2010). Babelomics: an integrative platform for the analysis of transcriptomics, proteomics and genomic data with advanced functional profiling. *Nucleic Acids Res.* **38**, W210-W213.
Mincheva-Nilsson, L. and Baranov, V. (2010). The role of placental exosomes in reproduction. Am. J. Reprod. Immunol. **63**, 520-533.
Moreno-Moya, J. M., Vilella, F., Martinez, S., Pellicer, A. and Simón, C. (2014). The transcriptomic and proteomic effects of ectopic overexpression of miR-30d in human endometrial epithelial cells. *Mol. Hum. Reprod.* **20**, 550-566.
Ng, Y. H., Rome, S., Jalabert, A., Forterre, A., Singh, H., Hincks, C. L. and Salamonsen, L. A. (2013). Endometrial exosomes/microvesicles in the uterine microenvironment: a new paradigm for embryo-endometrial cross talk at implantation. *PLoS ONE* **8**, e58502.
Niakan, K. K., Han, J., Pedersen, R. A., Simón, C. and Pera, R. A. R. (2012). Human pre-implantation embryo development. *Development* **139**, 829-841.
Özcan, S. (2014). MiR-30 family and EMT in human fetal pancreatic islets. *Islets* **1**, 283-285.
Paiva, P., Hannan, N. J., Hincks, C., Meehan, K. L., Pruysers, E., Dimitriadis, E. and Salamonsen, L. A. (2011). Human chorionic gonadotrophin regulates FGF2 and other cytokines produced by human endometrial epithelial cells, providing a mechanism for enhancing endometrial receptivity. *Hum. Reprod.***26**, 1153-1162.
Revel, A., Achache, H., Stevens, J., Smith, Y. and Reich, R. (2011). MicroRNAs are associated with human embryo implantation defects. *Hum. Reprod.* **26**, 2830-2840.
Sha, A.-G., Liu, J.-L., Jiang, X.-M., Ren, J.-Z., Ma, C.-H., Lei, W., Su, R.-W. and Yang, Z.-M. (2011). Genome-wide identification of micro-ribonucleic acids associated with human endometrial receptivity in natural and stimulated cycles by deep sequencing. *Fertil. Steril.* **96**, 150-155.e5.
Simón, C., Mercader, A., Frances, A., Gimeno, M. J., Polan, M. L., Remohí, J. and Pellicer, A. (1996). Hormonal regulation of serum and endometrial IL-1 alpha, IL-1 beta and IL-1ra: IL-1 endometrial microenvironment of the human embryo at the apposition phase under physiological and supraphysiological steroid level conditions. *J. Reprod. Immunol.* **31**, 165-184.
Simón, C., Gimeno, M. J., Mercader, A., O'Connor, J. E., Remohí, J., Polan, M. L. and Pellicer, A. (1997). Embryonic regulation of integrins beta 3, alpha 4, and alpha 1 in human endometrial epithelial cells in vitro. *J. Clin. Endocrinol. Metab.* **82**, 2607-2616.
Song, P.-P., Hu, Y., Liu, C.-M., Yan, M.-J., Song, G., Cui, Y., Xia, H.-F. and Ma, X. (2011). Embryonic ectoderm development protein is regulated by microRNAs in human neural tube defects. *Am. J. Obstet. Gynecol.* **204**, 544.e9-544.e17.
Thouas, G. A., Dominguez, F., Green, M. P., Vilella, F., Simón, C. and Gardner, D. K. (2014). Soluble ligands and their receptors in human embryo development and implantation. *Endocr. Rev.* **36**, er20141046.
Tian, T., Zhu, Y.-L., Hu, F.-H., Wang, Y.-Y., Huang, N.-P. and Xiao, Z.-D. (2013). Dynamics of exosome internalization and trafficking. *J. Cell. Physiol.* **228**, 1487-1495.
Tranguch, S., Daikoku, T., Guo, Y., Wang, H. and Dey, S. K. (2005). Molecular complexity in establishing uterine receptivity and implantation. *Cell. Mol. Life Sci.* **62**, 1964-1973.
Turchinovich, A., Weiz, L., Langheinz, A. and Burwinkel, B. (2011). Characterization of extracellular circulating microRNA. *Nucleic Acids Res.* **39**, 7223-7233.
Valadi, H., Ekström, K., Bossios, A., Sjöstrand, M., Lee, J. J. and Lötvall, J. O. (2007). Exosome-mediated transfer of mRNAs and microRNAs is a novel mechanism of genetic exchange between cells. *Nat. Cell Biol.* **9**, 654-659.
van der Gaast, M. H., Macklon, N. S., Beier-Hellwig, K., Krusche, C. A., Fauser, B. C. J. M., Beier, H. M. and Classen-Linke, I. (2009). The feasibility of a less invasive method to assess endometrial maturation-comparison of simultaneously obtained uterine secretion and tissue biopsy. *BJOG* **116**, 304-312.
Vilella, F., Ramirez, L., Berlanga, O., Martínez, S., Alamá, P., Meseguer, M., Pellicer, A. and Simón, C. (2013). PGE2 and PGF2α Concentrations in Human Endometrial Fluid as Biomarkers for Embryonic Implantation. *J. Clin. Endocrinol. Metab.* **98**, 4123-4132.
Yoshizawa, J. M. and Wong, D. T. W. (2013). Salivary MicroRNAs and oral cancer detection. *Methods Mol. Biol.* **936**, 313-324.

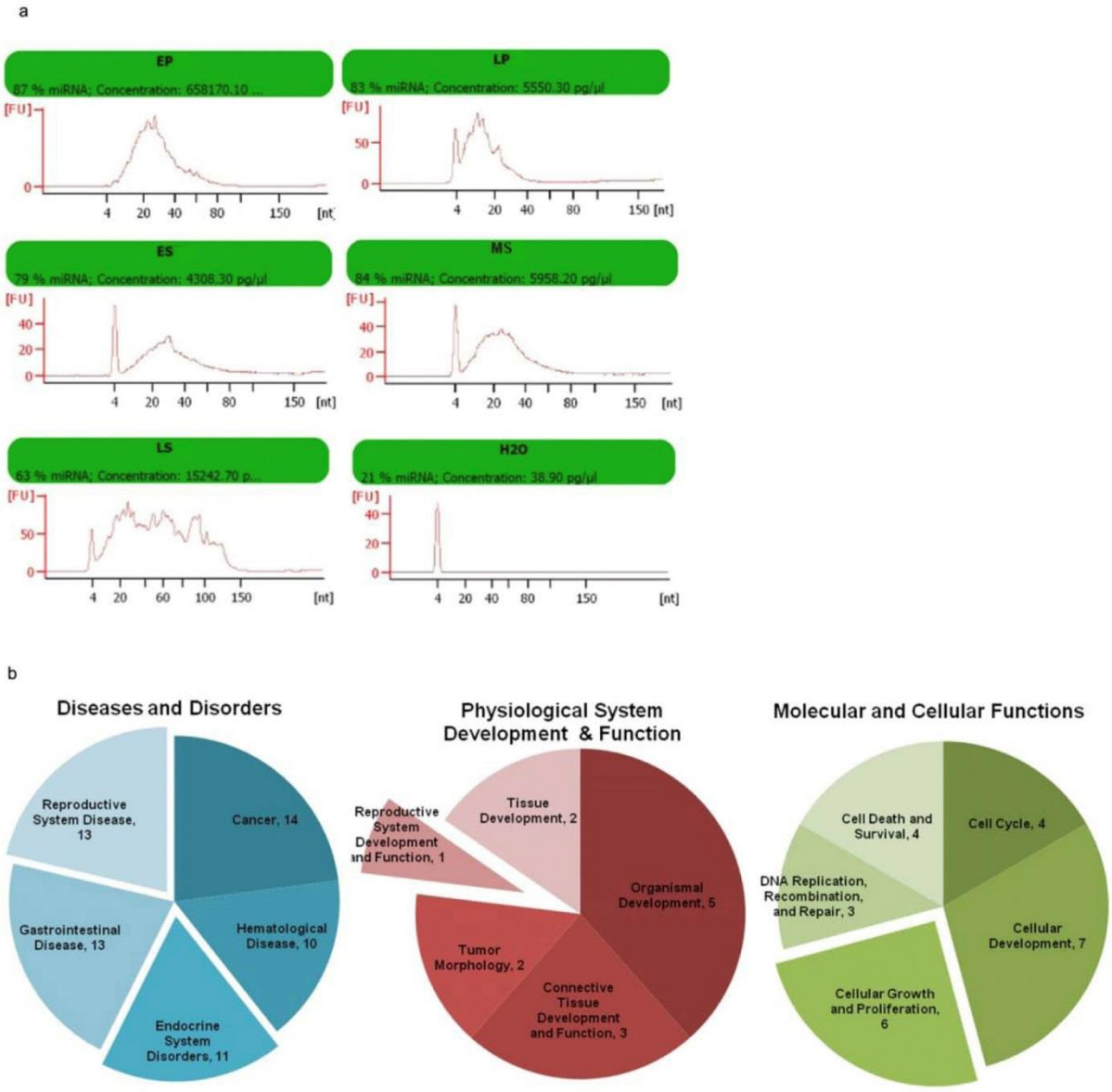

Supplementary Figure 1. Analysis of RNA content in endometrial fluid and evaluation of its biological function. (a) Small RNA content of endometrial fluid samples throughout the menstrual cycle determined using the Small RNA LabChip. (b) Functional classification of the microRNAs identified in endometrial fluid.

Development • Supplementary information

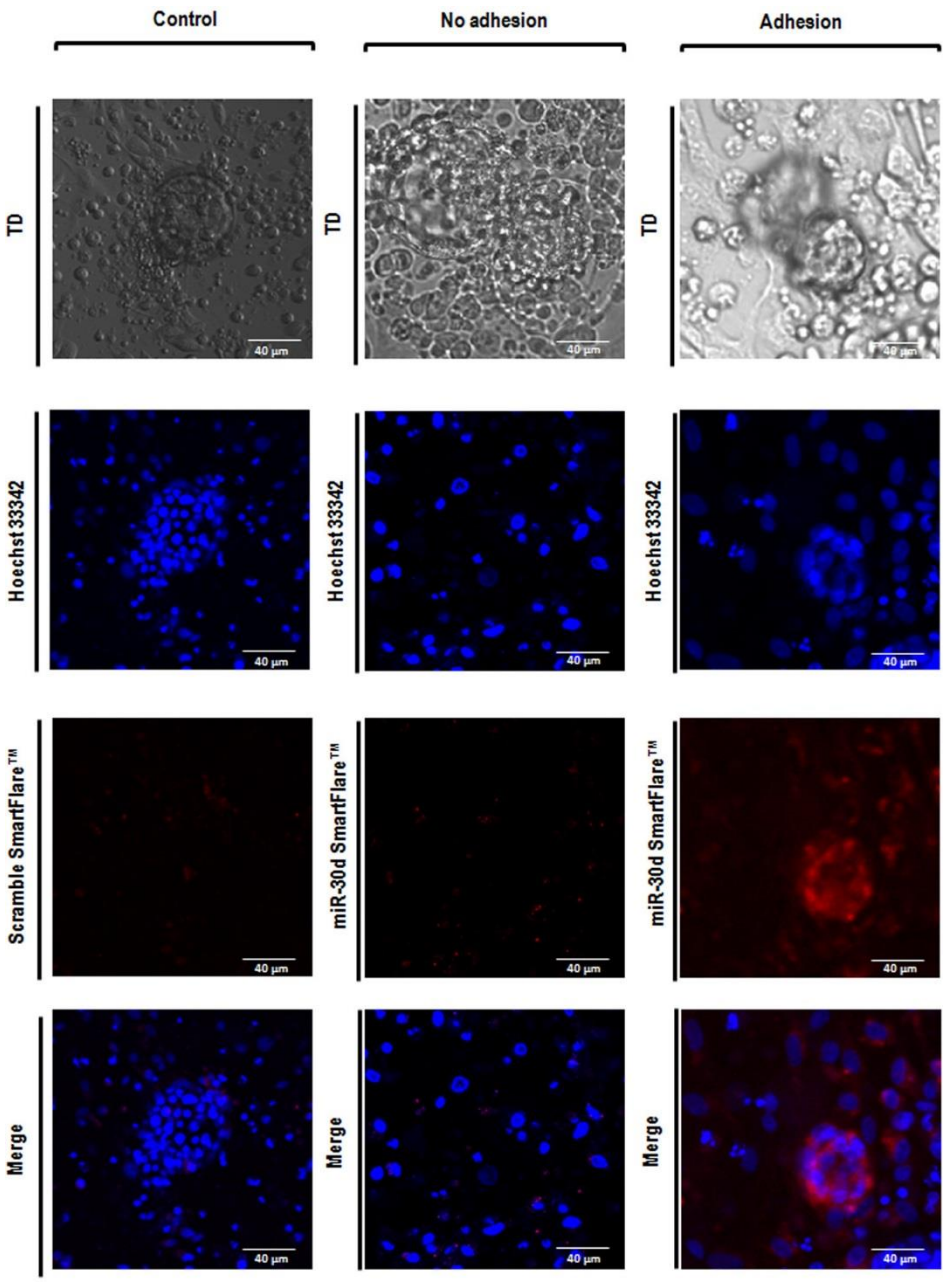

Supplementary Figure 2. Identification of hsa-miR-30d uptake from hEECs by mouse embryos (hECC focus). Confocal microscopy images show the projection in z of the plane of SmartFlare™-labeled-human epithelium (red) that was in contact with the mouse embryos shown in Fig. 5.

Development • Supplementary information

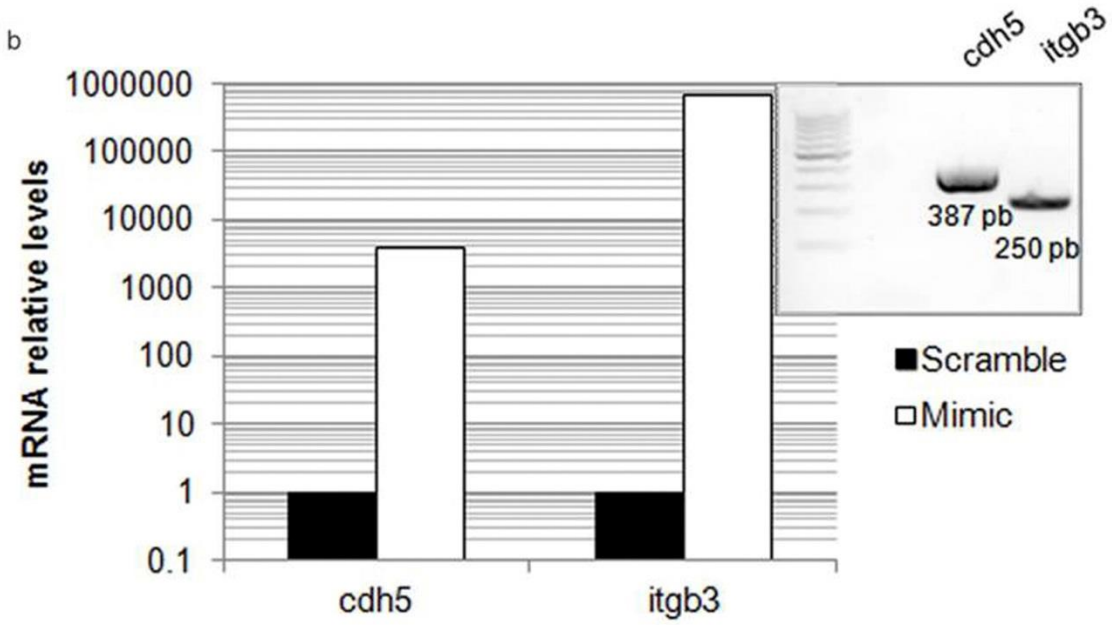

Supplementary Figure 3. Validation of transcriptomic gene expression in mouse embryos. Quantitative real-time PCR was used to validate the relative transcript abundance of the most significantly upregulated genes identified on the microarrays.

Development • Supplementary information

Supplementary Movie 1. Live animation showing the location of miR-30d in human luminal epithelium.

Development • Supplementary information

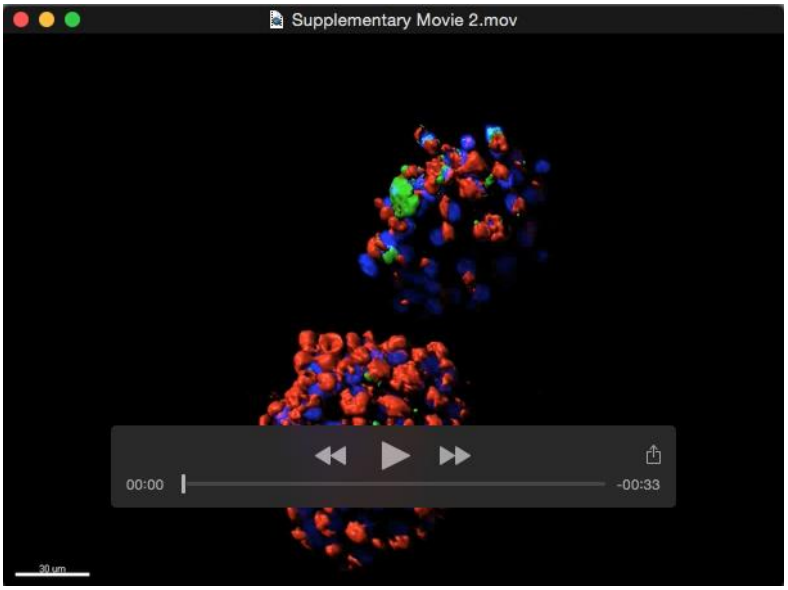

Supplementary Movie 2. Live animation showing a hatching mouse blastocyst treated with 400 nM Alexa488-scramble miRNA for 72 h (green).

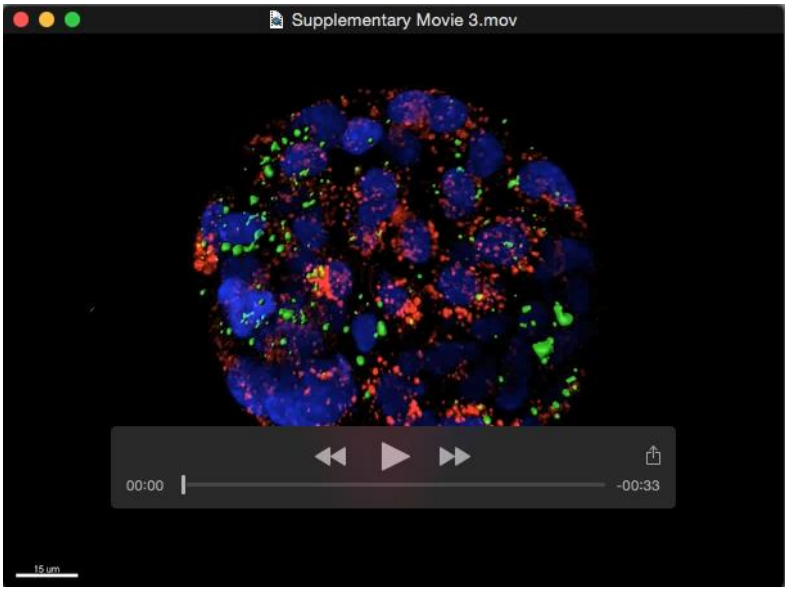

Supplementary Movie 3. Live animation showing a hatched blastocyst cultured with hEEC exosomes labeled with Vybrant DiO for 24 h (green).

Development • Supplementary information

Supplementary Table 1. Endometrial fluid sample parameters and primers for transcriptomic qPCR validation. (a) Endometrial fluid sample characteristics. (b) Primers used for validation in murine embryos of select transcripts identified through the transcriptomic analysis of human EF.

a

Menstrual cycle stage	Mean day of cycle ± SD	Mean age ± SD	%miRNA ± SD
Early proliferative (EP)	6.75 ± 1.25	37.25 ± 3.30	60.5% ± 12.87%
Late proliferative (LP)	12.5 ± 1.73	37 ± 5.77	48.75% ± 7.41%
Early secretory (ES)	16.25 ± 1.50	38.75 ± 3.09	40.5% ± 2.65%
Window of implantation (WOI)	20.75 ± 1.70	36 ± 3.60	64% ± 19.5%
Late secretory (LS)	31.5 ± 4.20	40 ± 3.82	45.25% ± 12.65

b

Gene		Sequence	Length, bp	Tm, °C	%GC	Self-complementarity
Cdh5	**Forward**	ATGGCAGGCCCTAACTTTCC	20	60.03	55.00	5.00
	Reverse	GTGCGAAAACACAGGCCAAT	20	59.97	50.00	4.00
Itgb3	**Forward**	GGGTACCAAGTTGGCCTCTC	20	60.04	60.00	7.00
	Reverse	ATCTCGATTACGGGACACGC	20	59.97	55.00	4.00
Gapdh	**Forward**	AACTCGGCCCCCAACACT	18	61.18	61.11	4.00
	Reverse	CCTAGGCCCCTCCTGTTATTATG	23	59.74	52.17	6.00

Development • Supplementary information

Supplementary Table 2. Data from expression arrays. Comparison between embryos treated with hsa-miR-30d inhibitor and control.

Click here to Download Table S2

Supplementary Table 3. Data from expression arrays. Comparison between embryos treated with hsa-miR-30d inhibitor and scramble.

Click here to Download Table S3

Supplementary Table 4. Data from expression arrays. Comparison between embryos treated with hsa-miR-30d and control.

Click here to Download Table S4

Supplementary Table 5. Data from expression arrays. Comparison between embryos treated with hsa-miR-30d and hsa-miR-30d inhibitor.

Click here to Download Table S5

Supplementary Table 6. Data from expression arrays. Comparison between embryos treated with hsa-miR-30d and scramble.

Click here to Download Table S6

Development • Supplementary information

Supplementary Table 7. Data from expression arrays. Comparison between embryos treated with scramble and control.

Click here to Download Table S7

Supplementary Table 8. Predicted targets of hsa-miR-30d in human and mouse.

Click here to Download Table S8

Supplementary Table 9. Predicted GO terms of the hsa-miR-30d targets in human and mouse.

Click here to Download Table S9

Supplementary Table 10. Predicted GO terms of the hsa-miR-30d targets in human and mouse that are implicated in embryonic processes.

Click here to Download Table S10

Development • Supplementary information